19th Australasian Tunnelling Conference – Acosta-Martínez, Stewart and Hudson-Smith (Eds.)

Thermal properties of the Triassic rock formations across the Sydney region for the use in tunnel ventilation design

J. W. Davidson & D. Saunsbury
WSP Australia Pty Limited, Sydney, Australia

A. Bidarmaghz
School of Civil and Environmental Engineering, Sydney, Australia

D. J. Och
WSP Australia Pty Limited, Sydney, Australia
School of Biological, Earth and Environmental Sciences, Sydney, Australia

ABSTRACT: The thermal properties of the geological formations that host tunnels are an important parameter in the design of tunnel ventilation systems, particularly for metro and high-speed rail systems. The heat generated in these tunnels is transferred through the tunnel lining and into the geological formations around the tunnels. The rate of heat transfer is influenced by the thermal properties of the ground surrounding the tunnel. The resultant tunnel wall temperatures and air temperatures inside the tunnel are therefore partially dependent on the ground thermal properties. Tunnelling in Sydney Basin region is predominantly in Triassic rock formations of the Narrabeen Group, Hawkesbury Sandstone, transitioning between the Mittagong Formation and Wianamatta Group shales in the central part of the basin. Investigations into thermal properties of the ground across the central and northern parts of the Sydney Basin were conducted for three underground rapid transit projects in Sydney. Testing of borehole samples was undertaken to determine the thermal conductivity and diffusivity of the variable ground conditions around the tunnels. This paper presents the results and analysis of that testing for the purpose of applying to the tunnel ventilation design of current and future tunnel projects. The measured mean thermal conductivity was 2.85 W/m.K and the mean thermal diffusivity was in the range of 1.88×10^{-6} to 1.51×10^{-6} m^2/s.

1 INTRODUCTION

Tunnel ventilation systems are essential components of underground rapid transit infrastructure, designed to manage both emergency scenarios—such as smoke control during fires—and everyday operational conditions, including the regulation of tunnel air temperatures. In high-frequency metro systems, substantial heat is generated from sources such as train braking and acceleration, onboard air conditioning systems, friction, and tunnel-mounted equipment. This heat must be effectively dissipated to maintain safe and comfortable conditions for passengers and equipment, making thermal interaction between tunnel air and the surrounding ground a critical consideration in ventilation system design.

One of the primary mechanisms for heat dissipation is the transfer of thermal energy from the tunnel air to the surrounding ground through the tunnel lining. The effectiveness of this process depends on several factors, including the temperature gradient, the thermal properties of the tunnel lining, and the thermal conductivity of the surrounding geological materials. In regions like the Sydney Basin, where underground rail alignments traverse a variety of sedimentary rock formations, understanding the thermal properties of these materials is vital for accurate thermal modelling and efficient ventilation system design.

Thermal conductivity of geological materials is influenced by a range of internal and external factors. Internally, mineral composition plays a key role—rocks rich in quartz, for example, typically exhibit higher conductivity than those with greater clay content. Pore fluids such as water can enhance conductivity due to the rocks high heat capacity, while rock structure, including

porosity and fracture networks, can impede heat flow by introducing less conductive air pockets. Externally, temperature and pressure also affect conductivity, with higher pressures generally increasing it, particularly in sedimentary rocks. Additionally, mineral grain size, lithology, density, and are all known to correlate with thermal conductivity, further complicating its prediction in heterogeneous rock masses.

However, detailed thermal characterisation of the ground is often overlooked during early design phases due to time and cost constraints. Designers frequently rely on generic reference values (e.g., Robertson, 1988), which may not accurately reflect the heterogeneous and anisotropic nature of local geological formations. This can lead to discrepancies in predicted versus actual tunnel air temperatures, potentially resulting in over- or under-designed ventilation systems.

To address this gap, recent underground rail projects in the Sydney Basin have incorporated targeted geotechnical investigations, including thermal conductivity testing of rock samples obtained from boreholes along proposed tunnel alignments. These tests provided localised thermal property data, enabling more accurate modelling of long-term heat transfer between tunnel air and the surrounding ground.

This paper presents the results of thermal conductivity testing conducted on borehole samples from several corridors across the upper Sydney Basin, including tests previously assessed in Saunsbury et al. (2017). It outlines the geological context of each corridor, details the testing methodology, and analyses the results to inform future tunnel ventilation design.

2 GEOLOGICAL CONDITIONS

The Sydney Basin is a structural and topographic basin extending from Batemans Bay to Lithgow and Raymond Terrace. It was infilled during the Permian and Triassic periods (298–200 million years ago) with thick sedimentary sequences deposited under fluvial and marine conditions (Herbert, 1983).

Minor deformation at the end of the Late Triassic, part of a broader tectonic phase continuing into the Paleogene, contributed to the formation of the Tasman Sea (Herbert & Helby, 1980; Och et al., 2009). This tectonism introduced dominant joints, faults, and igneous intrusions such as dykes and diatremes. Recent studies suggest these features may be influenced by deeper basement structures.

During the Last Glacial Maximum (~120,000 years ago), sea levels were ~100 m lower, shifting the coastline ~20 km eastward. Major rivers, including the Hawkesbury and Parramatta, incised deep valleys into the uplifted eastern margin. Subsequent Pleistocene and Holocene transgressive-regressive cycles led to alternating phases of sedimentation and erosion, producing under-consolidated deposits and complex stratigraphy.

The distribution and composition of these dominant rock formations are summarised to inform this study and guide infrastructure planning for major transport and tunnelling projects in the central Sydney Basin:

2.1 *Ashfield Shale*

The Ashfield Shale, the lowest formation of the Wianamatta Group, becomes increasingly prevalent along tunnel corridors toward Parramatta, where it dips gently westward and reaches thicknesses of up to 50 m. It transitions into the upper Minchinbury Sandstone and Bringelly Shale (excluded from this study) to the west and comprises four stratigraphic members:

- Mulgoa Laminite Member – Dark grey siltstone with light grey sandstone laminations
- Regentville Siltstone Member – Dark grey sideritic-banded siltstone
- Kellyville Laminite Member – Light grey siltstone with fine to medium sandstone laminations
- Rouse Hill Siltstone Member – Dark grey to black claystone-siltstone, slightly carbonaceous

These rocks are anisotropic, with reduced strength parallel to bedding. These rocks are slightly absorbent (avg. moisture ~3%) and contain 3–30% quartz, up to 20% carbonate clasts, and clay cement stained by iron oxides (up to 80%).

2.2 *Mittagong Formation*

Underlying Ashfield Shale, this ~6 m thick formation features alternating shale and sandstone beds, often disturbed by soft sediment deformation and bioturbation. It shares characteristics with Ashfield Shale and Hawkesbury Sandstone but is distinguished by dominant siltstone and finer sandstone facies, respectively.

2.3 *Hawkesbury Sandstone*

The Hawkesbury Sandstone is the predominant rock formation encountered at tunnel depth and is typically characterised as a medium- to coarse-grained sandstone comprising 50–80% quartz with clay (5–40%), secondary silica (up to 20%), and iron carbonate cement (0–15%, occasionally up to 35%). Pore space reaches 5%, and moisture content averages 6.8%. Three facies are identified:

- Massive sandstone facies,
- Cross bedded or sheet facies (well developed or indistinct/poorly developed), and
- Shale/siltstone interbed – Mudstone facies.

2.4 *Narrabeen Group*

Deposited in fluvial to shallow marine settings during the Early to Middle Triassic, this group features variable lithologies including sandstones, siltstones, shales, and claystones. Key formations include Terrigal, Patonga, Tuggerah, and Munmorah, along with Bald Hill Claystone, Newport, and Garie formations.

The Terrigal Formation is notably complex, with interbedded sandstone, siltstone, claystone, and breccia. Petrographic data show 33–67% quartz, 2–12% feldspar, 5–30% lithics, and 5–10% clay matrix, with minor silica or calcite cement. Coarse beds may have up to 6% pore space, while finer beds range from <1% to 3%. The lower Terrigal and upper Tuggerah Formations contain approximately 20% shale members, while the Patonga Claystone includes around 10% sandstone interbeds. These interbedded layers, often more weathered and clay-rich than the Hawkesbury Sandstone, present geotechnical challenges due to strength and the rocks variability.

3 GROUND THERMAL PROPERTIES

3.1 *Legacy values*

Thermal conductivity and thermal diffusivity are the parameters typically used to define ground thermal properties in a tunnel ventilation analysis model. These parameters are direct input for the Subway Environment Simulation (SES) program typically used for rail tunnel ventilation analysis. Legacy values of 1.80 W/m·K for conductivity and 1.15 m^2/s for diffusivity have been used as values for sandstone on several major infrastructure projects in Sydney, for the purpose of designing tunnel ventilation systems.

3.2 *Sample data*

Following a previous study into the sensitivity of tunnel air temperatures to thermal conductivity and diffusivity (Saunsbury et al., 2017), geotechnical borehole testing has been conducted for additional infrastructure projects in Sydney. These tests measured each sample's thermal resistivity (the inverse of conductivity), moisture content, and/or dry density. From this data, it is possible to assess the validity of the legacy values and recommend new values if necessary. For consistency and to ensure the applicability of these values to future projects, only results from the Hawkesbury sandstone samples are presented here.

Three sets of borehole tests were obtained. The first (Dataset 1) includes the sandstone sample results from the previous sensitivity study (Saunsbury et al., 2017). For Datasets 1 and 2, thermal resistivity testing was completed in accordance with IEEE Standard 442, ASTM Standard D5334 and Ausgrid NS130 Appendix K. Tests produced measurements for moisture content, thermal resistivity and density in Table 1 and Table 2. Some details of the Dataset 1 and 2 tests are unknown, such as the condition of the samples prior to testing and whether thermal paste was used to maximise heat transfer at any interface locations.

Dataset 3 was tested at the School of Civil and Environmental Engineering, UNSW, using a C-therm thermal conductivity analyser under ASTM D7984 guidelines. A thin layer of thermal paste was applied to the sensor area and sample surface to minimise the air gaps between the machine and sample. This maximises heat transfer and allows the most accurate measurement possible to be obtained, reproduced in Table 3. Samples were stored to retain as much in situ moisture as possible. Measured values are therefore indicative of the in situ thermal properties.

Table 1. Dataset 1 (Saunsbury et al., 2017).

Test ID	Moisture [% Dry Mass]	Pre-Dry Out Thermal Resistivity [Km/W]	Dry Density [kg/m^3]
01	1.0	0.73	2560
02	6.2	0.72	2200
03	5.9	0.78	2250
04	6.6	0.81	2200

Table 2. Dataset 2.

Test ID	Moisture [% Dry Mass]	Pre-Dry Out Thermal Resistivity [Km/W]	Dry Density [kg/m^3]
05	6.1	0.34	2370
06	3.1	0.54	2525
07	6.0	0.32	2400
08	3.9	0.43	2440
09	6.6	0.29	2290
10	6.0	0.29	2310
11	3.3	0.31	2310
12	6.6	0.40	2240
13	6.7	0.36	2280
14	3.9	0.29	2320
15	4.8	0.27	2320

Table 3. Dataset 3.

Test ID	Moisture [% Dry Mass]	Pre-Dry Out Thermal Resistivity [Km/W]	Dry Density [kg/m^3]
16	-	0.31	-
17	-	0.30	-
18	-	0.39	-
19	-	0.27	-
20	-	0.30	-
21	-	0.36	-
22	-	0.25	-
23	-	0.57	-
24	-	0.47	-
25	-	0.33	-
26	-	0.45	-
27	-	0.19	-
28	-	0.61	-
29	-	0.55	-

3.3 *Sample distribution*

Thermal conductivity was calculated as the inverse of thermal resistance for each sample. Distribution plots for each dataset are presented in Figure 1.

Datasets 2 and 3 feature similar distributions across a similar range of conductivity values, excluding an outlier in the Dataset 3 sample. The maximum Dataset 3 value of 5.19 W/m·K is classified as an outlier because it falls outside the range calculated by the 1.5IQR (interquartile range) method. This is true when Dataset 3 is considered by itself and combined with Dataset 2. It is therefore considered reasonable and conservative to exclude this value from the analysis. The mean of Dataset 2 is 2.98 W/m·K and the mean of Dataset 3 is 2.75 W/m·K, excluding the outlier.

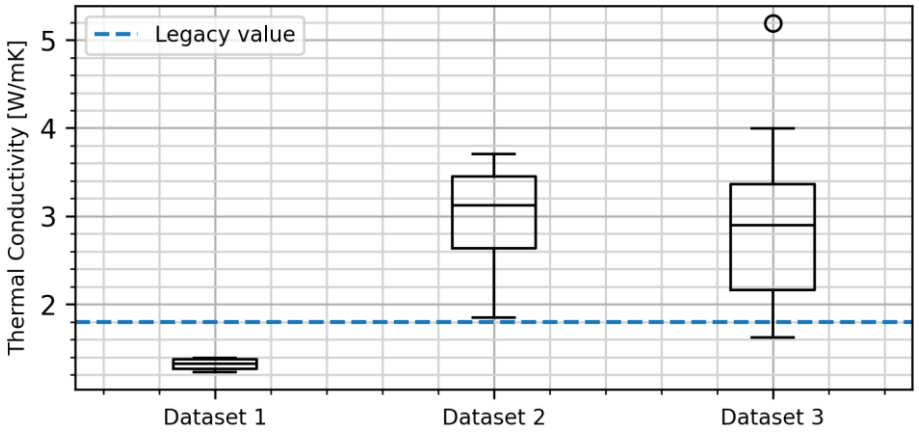

Figure 1. Sample thermal conductivity distributions for each dataset (median indicated by orange line).

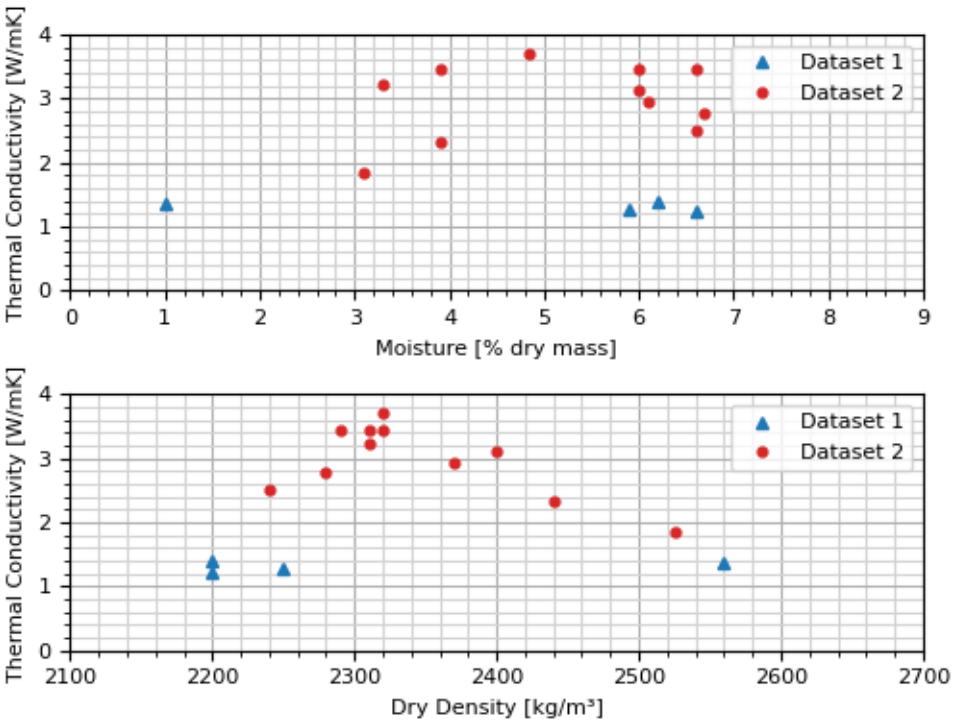

Figure 2. Thermal conductivity plotted against moisture and dry density for Dataset 1 and Dataset 2.

Compared to Datasets 2 and 3, Dataset 1 has significantly smaller conductivity values and a narrower distribution. The consistency between Datasets 2 and 3, and the differences from Dataset 1, suggest an irregularity in Dataset 1.

The available data does not explain the discrepancy between the Dataset 1 and the other datasets. As shown in Figure 2, Datasets 1 and 2 have a similar range of dry density and moisture content values. There is no apparent relationship between these and thermal conductivity in the samples. Differences in these properties between the datasets are therefore not a factor. Dataset 3 cannot be compared to Dataset 1 in this manner, as it does not include moisture or density measurements. Unmeasured parameters may explain the difference, such as gain size or mineralogical composition. Differences in testing conditions, as detailed in Section 3.2, are hypothesised to be more likely explanations for the inconsistency. Dataset 1 had unrecorded sample storage conditions, potentially leading to desiccation and artificially low conductivity.

Based on Dataset 1, which was the only available data at the time, the previous study (Saunsbury et al., 2017) found the sample conductivity values were substantially lower than the legacy value. Relative to Datasets 2 and 3, the legacy value of 1.80 W/m·K is however lower; the minimum value for Dataset 2 is 1.85 W/m·K and the minimum value for Dataset 3 is 1.63 W/m·K.

3.4 *Exploratory data analysis*

A Python script was used to test for any statistically significant differences between the thermal conductivity distributions of Datasets 2 and 3. A Shapiro-Wilk test was first used to test for normality, given the small samples sizes, with a null hypothesis that the datasets are normally distributed and a threshold value of 0.05. The p-values are given in Table 4. The same test was conducted for Dataset 2's moisture and dry density values (Table 5).

Moisture content's p-value is marginally above 0.05, while the others greatly exceed the threshold. All null hypotheses can therefore be accepted. As Dataset 3 does not contain moisture or density data, the same analysis was not performed for these parameters in Dataset 3.

Statistically significant differences in conductivity distribution between Datasets 2 and 3 were tested for. A two-sample t-test and Levene's test were selected. The null hypothesis supposed equal sample mean and variance between the datasets. The p-values are given in Table 6. Again, these exceed 0.05. This confirms the visual observations made in Section 3.3: Datasets 2 and 3 have conductivity normal distributions which are not different to a statistically significant degree.

To derive thermal conductivity and diffusivity values for use in future projects, the two datasets can therefore be considered together.

Table 4. Shapiro-Wilk p-values for Datasets 2 and 3 thermal conductivity values.

Dataset	Shapiro-Wilk p-value
2	0.4619
3	0.5325

Table 5. Shapiro-Wilk p-values for Dataset 2 moisture and dry density values.

Parameter	Shapiro-Wilk p-value
Moisture content	0.0501
Dry density	0.2346

Table 6. T-test and Levene p-values for a comparison of Datasets 2 and 3 thermal conductivity values.

Test	p-value
T-test for equal mean	0.1610
Levene's test for equal variance	0.2551

3.5 *Thermal diffusivity derivation*

As in Saunsbury et al. (2017) estimates of the thermal diffusivity of the samples in situ were calculated using thermal conductivity, wet bulk density, and specific heat capacity.

$$a = \frac{k}{\rho c_p} \quad (1)$$

Where;
a : thermal diffusivity (m^2/s)
k : thermal conductivity (W/m·K)
ρ : density (kg/m^3)
c_p : specific heat capacity (J/kg.K)

In situ wet bulk density was estimated using sample moisture content and dry density. Although thermal diffusivity cannot be directly derived from the sample data, Saunsbury et al. (2017) indicated that tunnel air temperatures are less sensitive to this parameter compared to thermal conductivity. This study adopted the same approach as Saunsbury et al. (2017) for estimating thermal diffusivity for the sensitivity study.

A range of specific heat capacities for sandstone is provided in Konakova et al. (2013) and included below in Table 7. Using the minimum and maximum values in this range, upper and lower estimates for thermal diffusivity were calculated for each sample, respectively.

Thermal diffusivity could not be calculated for the Dataset 3, as sample measurements for moisture and density were unavailable. Dataset 1 was excluded, as discussed previously.

Table 7. Specific heat capacity values from Konakova et al (2013)

Dataset value	Specific heat capacity [J/kgK]
Minimum	645.62
Maximum	801.23

3.6 *Thermal conductivity and diffusivity values to be adopted for future use*

Because the datasets are normally distributed, bell curves were generated using the sample mean and variance (Figure 3). The combined thermal conductivity dataset considered all samples from Datasets 2 and 3, excluding the outlier in Dataset 3. The same was done for thermal diffusivity. Separate curves were produced for the lower and upper estimates. Dataset 1 samples were excluded when generating the distributions. Summary statistics are provided in Table 8.

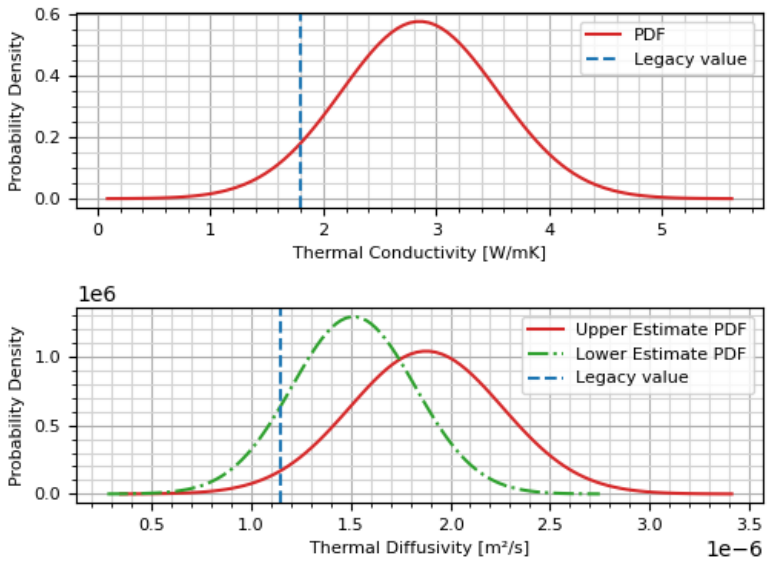

Figure 3. Probability distributions for thermal conductivity and thermal diffusivity.

Table 8. Derived means and 95th percentile values for thermal conductivity and diffusivity.

Parameter	Thermal conductivity [W/m·K]	Thermal diffusivity (upper estimate) [m^2/s]	Thermal diffusivity (lower estimate) [m^2/s]
Mean	2.85	1.88×10^{-6}	1.51×10^{-6}
95th percentile*	1.71	2.50×10^{-6}	2.03×10^{-6}

*For thermal conductivity, "95th percentile" refers to the lower end of the distribution, as this is worse for tunnel air temperatures.

The legacy conductivity value is conservative relative to the borehole sample data. This suggests a higher value may be more appropriate for the design of tunnel ventilation systems which would lead to potentially lower predicted tunnel air temperatures. Conversely, estimated thermal diffusivity values are more conservative relative to the legacy value. However, as found in Saunsbury et al. (2017), tunnel air temperatures are not as sensitive to this parameter.

4 CONCLUSIONS

This study evaluated the thermal properties of different rocks relevant to tunnel ventilation design in the Sydney Basin. Analysis of three datasets revealed that Datasets 2 and 3 produced consistent thermal conductivity values, significantly higher than both Dataset 1 and the legacy value of 1.80 W/m·K. Statistical testing confirmed no significant difference between Datasets 2 and 3, indicating reliability of both datasets. The discrepancy with Dataset 1 likely stems from unaccounted testing conditions or sample characteristics. Consequently, the legacy conductivity value appears conservative, and updated values from Datasets 2 and 3 could be considered more appropriate for future tunnel ventilation design. Thermal diffusivity remains a secondary factor, estimated using established methods.

5 REFERENCES

Herbert, C., 1983. Sydney Basin stratigraphy, Geological Survey of New South Wales, Department of Mineral Resources, Sydney.

Herbert, C. and Helby, R., 1980. A guide to the Sydney Basin, Bulletin 26. Geological Survey of New South Wales, Department of Mineral Resources, Sydney, 603 pp.

Konakova, D., Vejmelkova, E. and Cerny, R., 2013. Thermal properties of selected sandstones. Czech Technical University, Prague.

Och, D.J., Offler, R., Zwingmann, H., Braybrooke, J. and Graham, I.T., 2009. Timing of brittle faulting and thermal events, Sydney region: association with the early stages of extension of East Gondwana. Australian Journal of Earth Sciences, 56(7): 873 - 887.

Robertson, E.C., 1988. Thermal properties of rocks, United States Department of the Interior - Geological Survey, Reston, Virginia.

Saunsbury, D., Fernandes, D. and Och, D.J., 2017. A Preliminary Study on the Thermal Properties of the Ground under Sydney Harbour and the Sensitivity of Tunnel Air Temperatures, 16TH Australasian Tunnelling Conference. ATS, Sydney, pp. 8.